



Synthesis, crystal structure and optical properties of the new lead fluoride borate— $\text{Pb}_2\text{BO}_3\text{F}$

Wenwu Zhao^{a,b}, Shilie Pan^{a,*}, Jian Han^a, Jiyong Yao^c, Yun Yang^{a,b}, Junjie Li^{a,b}, Min Zhang^{a,b}, Lian Han Zhang^d, Yin Hang^d

^a Xinjiang Key Laboratory of Electronic Information Materials and Devices, Xinjiang Technical Institute of Physics & Chemistry, Chinese Academy of Sciences, 40-1 South Beijing Road, Urumqi 830011, China

^b Graduate School of the Chinese Academy of Sciences, Beijing 100049, China

^c Technical Institute of Physics & Chemistry, Beijing 100049, China

^d Shanghai Institute of Optics & Fine Mechanics, Chinese Academy of Sciences, Shanghai 201800, China

ARTICLE INFO

Article history:

Received 18 May 2011

Received in revised form

10 August 2011

Accepted 18 August 2011

Available online 31 August 2011

Keywords:

$\text{Pb}_2\text{BO}_3\text{F}$

Synthesis

Crystal structure

Borate

ABSTRACT

A new compound, $\text{Pb}_2\text{BO}_3\text{F}$, has been grown by high temperature solution method from the $\text{PbO-PbF}_2\text{-B}_2\text{O}_3$ system for the first time. The crystal structure of this compound has been identified by single crystal X-ray diffraction analysis. It crystallizes in the hexagonal system, space group $P6_3/m$ (No. 176) with unit-cell parameters $a=7.2460(3)$ Å, $c=14.5521(17)$ Å, $Z=6$, $V=661.69(9)$ Å³. Its structure was solved by the direct methods and refined to $R_1=0.0163$ and $wR_2=0.0367$. The structure of $\text{Pb}_2\text{BO}_3\text{F}$ consists of the distorted PbO_3F_2 groups and BO_3 triangles, which are all symmetric with each other in the gestalt structure to the extent that the $\text{Pb}_2\text{BO}_3\text{F}$ compound crystallizes in the symmetric space group. The powder X-ray diffraction pattern of the $\text{Pb}_2\text{BO}_3\text{F}$ has been measured. The BO_3 functional groups presented in the sample were identified by FTIR spectrum. The DTA curve of $\text{Pb}_2\text{BO}_3\text{F}$ suggests that $\text{Pb}_2\text{BO}_3\text{F}$ melts congruently at 448 °C.

© 2011 Elsevier Inc. All rights reserved.

1. Introduction

The design and synthesis of new materials with large macroscopic nonlinearities has been receiving more and more attention. Especially research in borate crystals has been conducted for the past few decades and it remains strong to this date due to their promising physical properties, such as their interesting nonlinear optical, transparency to a wide range of wavelengths, high laser damage tolerance, piezoelectric, luminescent and other useful properties for technical applications [1–6]. Based on the theoretical model put forward by Wu and Chen [7], several new NLO crystals in the borate series have been developed over the years, typical representatives being $\beta\text{-BaB}_2\text{O}_4$ [8], and the subsequent discoveries of several other borate compounds, for example LiB_3O_5 [9], CsB_3O_5 [10], $\text{CsLiB}_6\text{O}_{10}$ [11], $\text{Sr}_2\text{Be}_2\text{B}_2\text{O}_7$ [12], $\text{KBe}_2\text{-BO}_3\text{F}_2$ [13], and so on.

According to the previous research work, lead borates are of special interest in the search for materials, since some of these compounds have pronounced nonlinear optical properties [14], such as PbB_4O_7 [15], $\text{Pb}_6\text{B}_{11}\text{O}_{18}(\text{OH})_9$ [14], $\text{Pb}[\text{B}_8\text{O}_{11}(\text{OH})_4]$ [16], $\text{Pb}_4\text{Bi}_3\text{B}_7\text{O}_{19}$ [17], $\text{Pb}_2\text{B}_5\text{O}_9\text{X}$ ($\text{X}=\text{Cl}, \text{Br}, \text{I}$) [18], $\text{Pb}[\text{B}_5\text{O}_8(\text{OH})] \cdot 1.5\text{H}_2\text{O}$

[19], and so on. The selection of lead borates for the investigation of structure–property relationships is of special interest because of the highly asymmetric bonding feature typical for a lead atom due to the stereo-effect of the lone pair of Pb^{2+} [20]. In our experiments, the lead fluoride borate crystals were attempted to synthesize from the $\text{PbO-PbF}_2\text{-B}_2\text{O}_3$ system. In this paper, we have obtained a new lead fluoride borate compound with a composition of $\text{Pb}_2\text{BO}_3\text{F}$. It crystallizes in the hexagonal system, space group $P6_3/m$ (No. 176) with unit-cell parameters $a=7.2460(3)$ Å, $c=14.5521(17)$ Å, $Z=6$, $V=661.69(9)$ Å³. Herein its synthesis, crystal structure and some optical properties will be reported.

2. Experimental section

2.1. Single-crystal growth

Single crystals of the $\text{Pb}_2\text{BO}_3\text{F}$ compound were obtained from a mixture of PbO (99.0%, Tianjing Baishi Chemical Co.), PbF_2 (99.5%, Tianjin Chemical Co.) and H_3BO_3 (99.5%, Beijing Chemical Co.) in the molar ratio of 3:2:2 by the high temperature solution method. The starting materials were weighed and melted in a Pt crucible in several batches. The crucible position was fixed at the center of the resistance-heated furnace. The temperature of the furnace was controlled within 0.1–1 °C by an AI-708 P controller and

* Corresponding author. Fax: + 86 991 3838957.

E-mail address: slpan@ms.xjb.ac.cn (S. Pan).

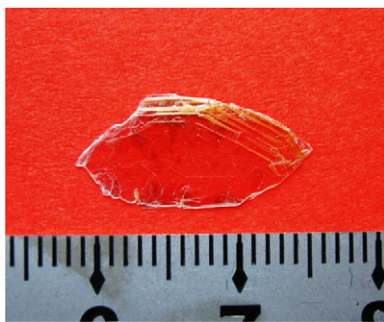


Fig. 1. Picture of the $\text{Pb}_2\text{BO}_3\text{F}$ crystals.

a Pt/Pt–Rh thermocouple. The temperature was raised at about $50\text{ }^\circ\text{C/h}$ – $50\text{ }^\circ\text{C}$ above the melting point and held for 15 h to ensure the solution mixed homogeneously. Then the solution was cooled down to $387\text{ }^\circ\text{C}$, and a platinum wire was rapidly introduced into the furnace and dipped into the solution, which was then followed by a slow cooling down to $380\text{ }^\circ\text{C}$ at a rate of $2\text{ }^\circ\text{C/day}$ and followed by cooling to room temperature at $20\text{ }^\circ\text{C/h}$. Then, colorless crystals with centimeter grade could be obtained from the solution for the structure determination. The picture of the $\text{Pb}_2\text{BO}_3\text{F}$ crystals is shown in Fig. 1.

2.2. Single-crystal X-ray crystallography

The crystal structure of $\text{Pb}_2\text{BO}_3\text{F}$ was determined by standard crystallographic methods: A clear light crystal was mounted on a thin glass fiber with silicone oil. It was investigated by SMART APEX II Single-Crystal diffractometer using monochromatic Mo $K\alpha$ radiation ($\lambda=0.71073\text{ \AA}$) at $296(2)\text{ K}$ and integrated with the SAINT-Plus program [21]. All refinements were completed with programs from the SHELXTL crystallographic software package [22]. The structure was solved by direct methods.

At first, the crystal structure of $\text{Pb}_2\text{BO}_3\text{F}$ was solved in space group $P6_3/m$ (No. 176), which was recommended by the SHELXTL crystallographic software package with initial heavy-atom positions, lead, located by direct methods. The other atoms were located by subsequent cycles of refinements and Fourier difference maps. Then, we obtained the formula of the compound. Then, we check the result by the program PLATON [23]. Unfortunately it suggested the presence of m and c faces, and the structure solution was restarted in space group $P6_3/mcm$ (No. 193). However, we check the data in detail by the APEX II software and then find that it is a merohedral twin in space group $P6_3/m$ with twin ratio of $0.63/0.37$. So, we solved the crystal structure in space group $P6_3/m$. The final full-matrix least-squares refinement was on F_0^2 with data having $F_0^2 \geq 2\sigma(F_0^2)$ and all atoms were refined with anisotropic thermal parameters. The final refinement was converged with $R_1=0.0163$ and $wR_2=0.0367$. The final difference Fourier synthesis may have shown maximum and minimum peaks at 1.003 and -0.955 e/\AA^3 , respectively.

The crystallographic data, the details of X-ray data collections, and refinement parameters for the structure determination are presented in Table 1. The final atomic coordinates with equivalent isotropic displacements and bond valence analysis for $\text{Pb}_2\text{BO}_3\text{F}$ are given in Table 2. Selected bond distances (\AA) and angles (deg.) for $\text{Pb}_2\text{BO}_3\text{F}$ are given in Table 3.

2.3. Solid-state synthesis

Polycrystalline powder samples of $\text{Pb}_2\text{BO}_3\text{F}$ were synthesized by solid-state reaction of a stoichiometric mixture of PbO , PbF_2

Table 1
Crystal data and structure refinement for $\text{Pb}_2\text{BO}_3\text{F}$.

Empirical formula	$\text{Pb}_2\text{BO}_3\text{F}$
Formula weight	429.19
Temperature	296(2) K
Crystal system	Hexagonal
Space group	$P6_3/m$
Unit cell dimensions	$a=7.2460(3)\text{ \AA}$ $b=7.2460(3)\text{ \AA}$ $c=14.5521(17)\text{ \AA}$
Z, volume	$6661.69(9)\text{ \AA}^3$
Density (calculated)	7.411 g/cm^3
Absorption coefficient	$76.129/\text{mm}$
$F(0\ 0\ 0)$	1212
Crystal size	$0.291 \times 0.254 \times 0.024\text{ mm}^3$
Theta range for data collection	1.40 to 27.42°
Index ranges	$-9 \leq h \leq 9$, $-9 \leq k \leq 9$, $-18 \leq l \leq 18$
Reflections collected	10,023
Independent reflections	$530[R(\text{int})=0.0499]$
Completeness to theta= 24.99	100.0%
Absorption correction	Numerical
Max. and min. transmission	0.2889 and 0.0071
Data/restraints/parameters	530/0/38
Goodness-of-fit on F^2	1.332
Final R indices [$F_0^2 > 2\sigma(F_0^2)$]	$R_1=0.0163$, $wR_2=0.0367$
R indices (all data)	$R_1=0.0176$, $wR_2=0.0370$
Largest diff. peak and hole	1.003 and -0.955 e \AA^{-3}

Table 2

Atomic coordinates, equivalent isotropic displacement parameters ($\text{\AA}^2 \times 10^3$) and bond valence analysis for $\text{Pb}_2\text{BO}_3\text{F}$. U_{eq} is defined as one-third of the trace of the orthogonalized U_{ij} tensor.^{a,b}

Atom	x	y	z	U_{eq}	BVS
Pb(1)	0.316(1)	0.991(1)	0.606(1)	14(1)	2.121
B(1)	0.0091(12)	0.642(12)	3/4	18(2)	2.901
O(1)	0.0014(9)	0.448(7)	3/4	17(1)	2.080
O(2)	0.0105(5)	0.735(6)	0.667(3)	17(1)	2.211
F(1)	1/3	2/3	0.562(5)	30(2)	0.798
F(2)	0	1	1/2	28(2)	0.720

^a Bond valences calculated with the program Bond Valence Calculator Version 2.00, Hormillosa, C., Healy, S., Stephen, T. McMaster University (1993).

^b Valence sums calculated with the formula: $S_i = \exp[(R_0 - R_i)/B]$, where S_i = valence of bond "i" and $B=0.37$.

Table 3

Selected bond distances (\AA) and angles (deg.) for $\text{Pb}_2\text{BO}_3\text{F}$.

Pb(1)–O(2)	2.241(4)	B(1)–O(1)	1.378(8)
Pb(1)–O(1)#1	2.2915(18)	B(1)–O(2)#3	1.386(5)
Pb(1)–O(2)#2	2.438(3)	B(1)–O(2)	1.386(5)
Pb(1)–F(1)	2.4938(18)	O(1)–B(1)–O(2)#3	119.0(3)
Pb(1)–F(2)	2.7882(2)	O(1)–B(1)–O(2)	119.0(3)
O(2)–Pb(1)–O(1)#1	83.26(16)	O(2)#3–B(1)–O(2)	122.0(6)
O(2)–Pb(1)–O(2)#2	92.76(19)	O(2)–Pb(1)–F(2)	75.72(9)
O(1)#1–Pb(1)–O(2)#2	83.16(15)	O(1)#1–Pb(1)–F(2)	146.98(10)
O(2)–Pb(1)–F(1)	79.42(12)	O(2)#2–Pb(1)–F(2)	72.87(9)
O(1)#1–Pb(1)–F(1)	92.4(2)	F(1)–Pb(1)–F(2)	108.15(11)
O(2)#2–Pb(1)–F(1)	171.42(16)		

Note: Symmetry transformations used to generate equivalent atoms: #1 $-x+y, -x+1, z$; #2 $-y+1, x-y+2, z$; #3 $x, y, -z+3/2$; #4 $-y+1, x-y+1, z$; #5 $-y+1, x-y+1, -z+3/2$; #6 $-x+y-1, -x+1, z$.

and H_3BO_3 powders. The starting materials were ground and packed into Pt crucible, which were slowly heated to $350\text{ }^\circ\text{C}$ and held for about 5 h to eliminate the water. Then the reaction

mixture were elevated to 450 °C and sintered at this temperature for 48 h with several intermediate grindings. In this way, vermeil products were obtained for the determination of powder X-ray diffraction and some optical measurement.

2.4. Powder X-ray diffraction

X-ray diffraction investigations on polycrystalline $\text{Pb}_2\text{BO}_3\text{F}$ were carried out with a Bruker D8 advanced diffractometer equipped with a diffracted-beamed monochromator set for $\text{Cu K}\alpha$ ($\lambda=1.5418 \text{ \AA}$) radiation. The data were collected using a Ni-filtered Cu-target tube at room temperature in the 2θ range from 10° to 70° , with a scan step width of 0.01° , and a fixed counting time of 0.2 s/step. Fig. 2 shows the experimentally observed powder X-ray pattern and that simulated from the single-crystal structural data. As shown in Fig. 2, the curves are similar to each other except for some weak diffraction, and after repeated experiment, it is found that some small extra reflections in the observed pattern are attributed to the impurities.

2.5. Infrared spectrum

To analyze the presence of BO_3 group in the $\text{Pb}_2\text{BO}_3\text{F}$ compound qualitatively, the Fourier transform infrared (FTIR) spectrum was recorded in the range $400\text{--}4000 \text{ cm}^{-1}$ using the Shimadzu IR Affinity-1 infrared spectrometer. The sample was in pellet form in the KBr phase (5 mg of the sample and 500 mg of KBr). The characteristic transmission peaks were shown in Fig. 3.

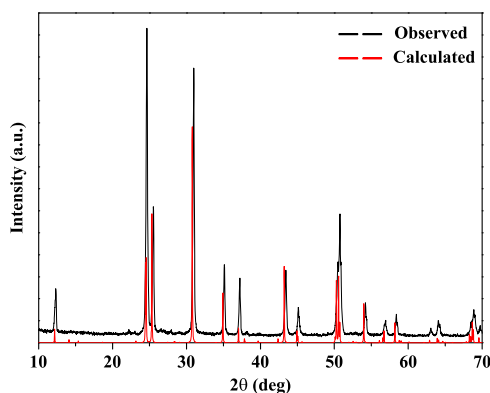


Fig. 2. Calculated and observed X-ray diffraction patterns of $\text{Pb}_2\text{BO}_3\text{F}$.

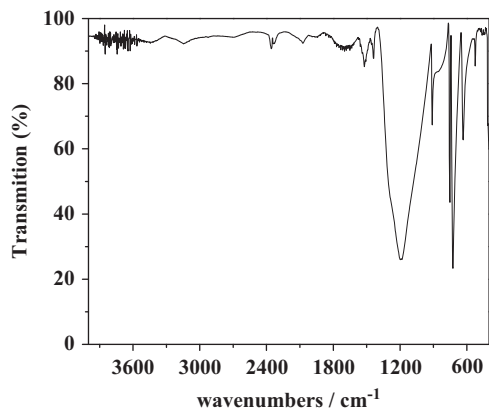


Fig. 3. IR spectrum of $\text{Pb}_2\text{BO}_3\text{F}$.

2.6. Diffuse reflectance spectrum

The SolidSpec-3700DUV spectrophotometer was used to measure the spectrum of the $\text{Pb}_2\text{BO}_3\text{F}$ powder samples over the range of 190 nm–2600 nm at room temperature.

2.7. Differential thermal analysis

The melting behaviors of $\text{Pb}_2\text{BO}_3\text{F}$ were investigated by differential thermal analysis (DTA) using a NETZSCH STA 449C simultaneous analyzer under static air. The sample and reference (Al_2O_3) were enclosed in Pt crucibles, heated from room temperature to 950 °C at a rate of $10^\circ\text{C}/\text{min}$.

3. Results and discussion

3.1. Crystal structure description

The reported material, $\text{Pb}_2\text{BO}_3\text{F}$, exhibits a three-dimensional crystal structure. The Pb atoms are in the five coordination environments bonded to three O atoms and two F atoms (see Fig. 4) to make up the distortional PbO_3F_2 polyhedra, with Pb–O bond distances ranging from $2.241(4) \text{ \AA}$ to $2.438(3) \text{ \AA}$ and the length between $2.494(18) \text{ \AA}$ and $2.788(2) \text{ \AA}$ for the Pb–F bond distances, respectively (see Table 3). From Fig. 4, we can know that every six PbO_3F_2 polyhedra are connected by one F(1) atom to form the symmetrical structure, and then the distortion of the PbO_3F_2 polyhedra is offset.

In the configuration shown in Fig. 5, the structure of $\text{Pb}_2\text{BO}_3\text{F}$ consists of the distortional PbO_3F_2 polyhedra and BO_3 triangles, which are connected to each other by the O(1) and O(2) atoms in the gestalt structure. From the figure, the PbO_3F_2 groups and BO_3 triangles are bonded to form the cage structure, which is connected only by F2 atoms along the c-axis. Since the weak bonding interactions between two adjacent cage structures, the crystal has a layered growth habit observed in the experiment (the crystal picture is shown in Fig. 1).

As is shown in Fig. 6, there are four orientations for the BO_3 triangles, and every two orientations are symmetric to each other to the extent that the $\text{Pb}_2\text{BO}_3\text{F}$ compound crystallizes in the

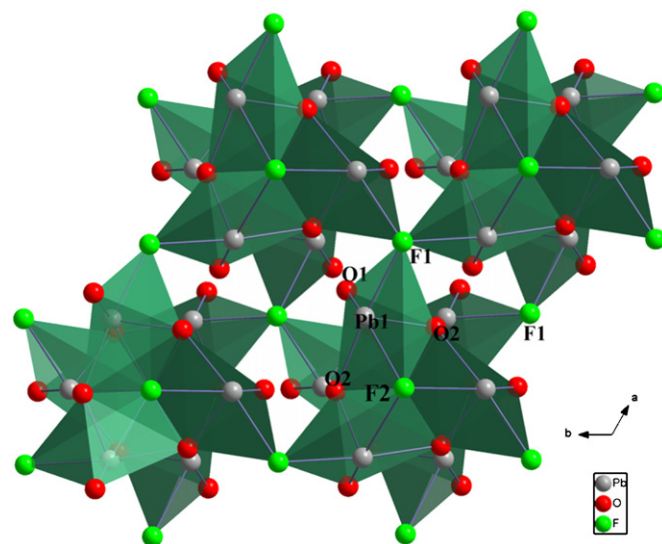


Fig. 4. PbO_3F_2 polyhedra (green polyhedra) in $\text{Pb}_2\text{BO}_3\text{F}$. (For interpretation of the references to color in this figure legend, the reader is referred to the web version of this article.)

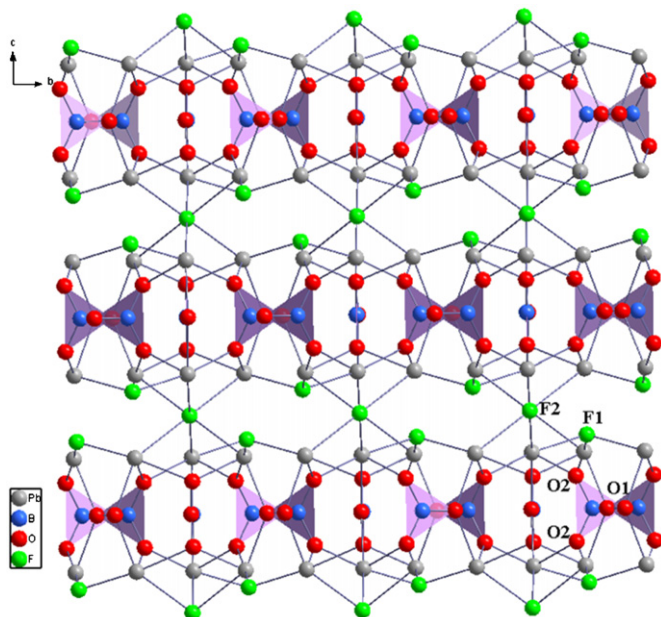


Fig. 5. Drawing of the structure of $\text{Pb}_2\text{BO}_3\text{F}$ viewed down the a -axis with the purple polyhedra are the BO_3 triangle groups. (For interpretation of the references to color in this figure legend, the reader is referred to the web version of this article.)

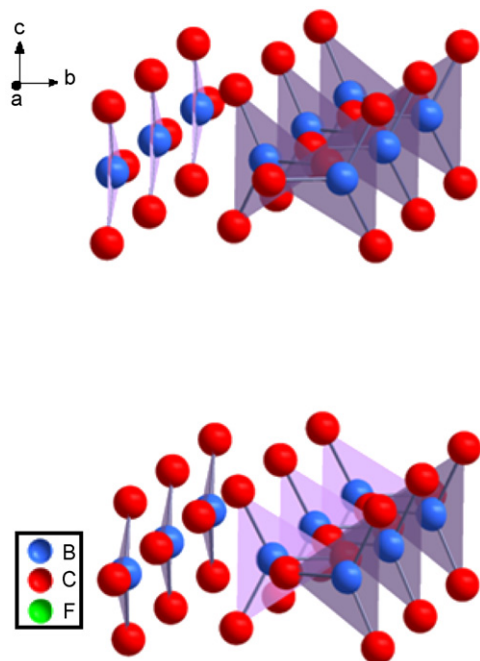


Fig. 6. Drawing of the four orientations of the BO_3 groups in the $\text{Pb}_2\text{BO}_3\text{F}$ compound.

symmetric space group. Meantime, all the BO_3 triangles consist of two O2 atoms and one O1 atom, with the length of the bond from 1.378(8) Å to 1.386(5) Å, and the mean distance for B–O bonds is 1.373 Å. The O–B–O angles are ranging from 119(3)° to 122(6)° with an average of 120°, which corresponds to the sp^2 hybridization of B atoms (see Table 3).

3.2. Infrared spectrum discussion

Fig. 3 shows the complete spectral region of the infrared spectrum between 400 and 4000 cm^{-1} . The broad peak observed

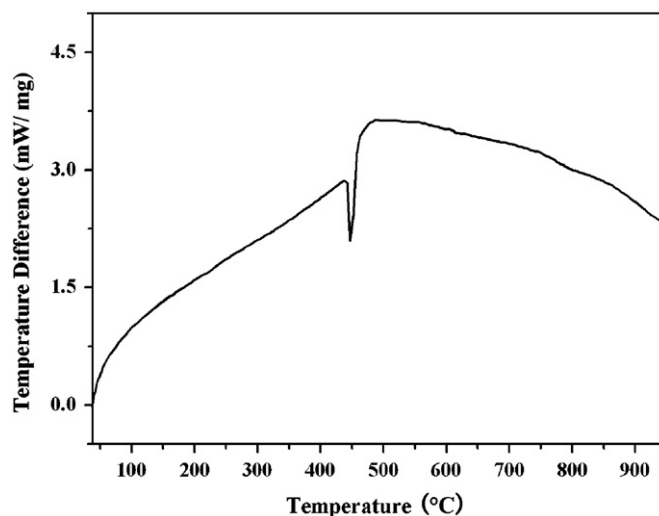


Fig. 7. DTA curve of $\text{Pb}_2\text{BO}_3\text{F}$.

in the 912 cm^{-1} and surveyed at the 1194 cm^{-1} , are characteristics of BO_3 asymmetric and symmetric stretching vibrations, respectively. The strong bands observed between 500 and 890 cm^{-1} at 752, 725, 635 and 525 cm^{-1} are assigned to the bending modes of triangular BO_3 groups. The result of this experiment is in agreement with other compounds containing BO_3 anionic groups [24,25].

3.3. Diffuse reflectance spectrum discussion

The UV–vis–NIR Diffuse-Reflectance spectrum between 190 and 2600 cm^{-1} for $\text{Pb}_2\text{BO}_3\text{F}$ polycrystalline powder is shown in Fig. S1 in the Supporting Information. It can be seen that a wide reflectance range is observed with the UV absorption edge at about 288 nm. There are no absorption peaks in the whole range of the spectrum.

3.4. Differential thermal analysis

The DTA curve of $\text{Pb}_2\text{BO}_3\text{F}$ is shown in Fig. 7. It shows one endothermic peak at 448 °C on the heating curve, which tentatively suggests that $\text{Pb}_2\text{BO}_3\text{F}$ melts congruently at 448 °C. To verify that $\text{Pb}_2\text{BO}_3\text{F}$ melts congruently, $\text{Pb}_2\text{BO}_3\text{F}$ crystal growth was tried in the stoichiometric mixture of PbO, PbF_2 and H_3BO_3 powders. In this experiment, the single crystals of the $\text{Pb}_2\text{BO}_3\text{F}$ compound were also obtained (see Fig. S2 in the Supporting Information), which further demonstrates that $\text{Pb}_2\text{BO}_3\text{F}$ is a congruently melting compound.

4. Conclusions

In this paper, we report a new lead fluoride borate compound, $\text{Pb}_2\text{BO}_3\text{F}$, it crystallizes in the hexagonal system, space group $P6_3/m$ (No. 167) with unit-cell parameters $a=7.2460(3)$ Å, $c=14.5521(17)$ Å, $Z=6$, $V=661.69(9)$ Å³. The structure of $\text{Pb}_2\text{BO}_3\text{F}$ consists of the distorted PbO_3F_2 polyhedra and BO_3 triangles. Every six PbO_3F_2 polyhedra are connected by one F(1) atom to form the symmetrical structure, and then the distortion of the PbO_3F_2 polyhedra is offset. Meantime, all the BO_3 are symmetric with each other in the gestalt structure to the extent that the $\text{Pb}_2\text{BO}_3\text{F}$ compound crystallizes in the symmetric space group. The powder X-ray diffraction pattern of the $\text{Pb}_2\text{BO}_3\text{F}$ has been measured, which was corresponding to the simulated from the single-crystal structural data. The BO_3 functional groups present

in the sample were identified by FTIR spectrum. The DTA curve of $\text{Pb}_2\text{BO}_3\text{F}$ suggests that $\text{Pb}_2\text{BO}_3\text{F}$ melts congruently at 448 °C.

Supplementary material: CCDC 423430 contains the supplementary crystallographic data of this paper. These data can be obtained free of charge from The Cambridge Crystallographic Data Centre via www.ccdc.cam.ac.uk/data_request/cif. The UV–vis–NIR Diffuse-Reflectance spectrum of $\text{Pb}_2\text{BO}_3\text{F}$ is shown in the Supporting Information.

Acknowledgment

This work is supported by Main Direction Program of Knowledge Innovation of Chinese Academy of Sciences (Grant no. KJCX2-EW-H03-03), the “National Natural Science Foundation of China” (Grant nos. 50802110, 21001114), the “One Hundred Talents Project Foundation Program” of Chinese Academy of Sciences, the “Western Light Joint Scholar Foundation” Program of Chinese Academy of Sciences, the “Open-end Foundation Program” of Key Laboratory of Electronic Information Materials and Devices of Xinjiang Uygur Autonomous Region of China (Grant no. xjys0901-2009-01) and Scientific Research Program of Urumqi of China (Grant no. G09212001).

Appendix A. Supporting information

Supplementary data associated with this article can be found in the online version at doi:10.1016/j.jssc.2011.08.024.

References

- [1] K. Prabha, B. Feng, H. Chen, G. Bhagavannarayana, P. Sagayaraj, *Mater. Chem. Phys.* 127 (2011) 79–84.
- [2] X. Meng, Y. Song, H. Hou, Y. Fan, G. Li, Y. Zhu, *Inorg. Chem.* 42 (2003) 1306–1315.
- [3] S. Wang, E.V. Alekseev, W. Depmeier, T.E. Ibrecht-Schmitt, *Inorg. Chem.* 50 (2011) 2079–2081.
- [4] G. Paramesh, R. Vaish, K.B.R. Varma, *J. Non-Cryst. Solids* 357 (2011) 1479–1484.
- [5] E.R. Shaaban, *Physica B* 406 (2011) 406–411.
- [6] A. Haberer, R. Kaindl, O. Oeckler, H. Huppertz, *J. Solid State Chem.* 183 (2010) 1970–1979.
- [7] K. Wu, C. Chen, *Appl. Phys.* A54 (1992) 209–220.
- [8] C.T. Chen, Y.C. Wu, A. Jiang, G. You, *Sci. Sin. B* 15 (1985) 235.
- [9] C. Chen, Y. Wu, A. Jiang, B. Wu, G. You, R. Li, S. Lin, *J. Opt. Soc. Am. B* 6 (1989) 616.
- [10] T. Sasaki, Y. Mori, M. Yoshimura, Y.K. Yap, T. Kamimura, *Mater. Sci. Eng., R* 30 (2000) 1.
- [11] Y. Mori, I. Kuroda, S. Nakajima, T. Sasaki, S. Nakai, *Appl. Phys.* 34 (1995) 296.
- [12] C. Chen, Y. Wang, B. Wu, K. Wu, W. Zeng, L. Yu, *Nature* 26 (1995) 322–324.
- [13] C. Chen, Z. Xu, D. Deng, J. Zhang, G.K.L. Wong, B. Wu, N. Ye, D. Tang, *Appl. Phys. Lett.* 68 (1996) 2930.
- [14] P. Wang, Z. Liu, *Thermochim. Acta* 515 (2011) 91–95.
- [15] K.S. Bartwal, R. Bhatt, S. Kar, V.K. Wadhawan, *Mater. Sci. Eng., B* 85 (2001) 76–79.
- [16] G. Wang, Y. Sun, G. Yang, *J. Solid State Chem.* 179 (2006) 398–403.
- [17] N.S. Shuster, M.I. Zargarova, G.K. Abdullaev, *Inorg. Chem.* 7 (1985) 1073–1074.
- [18] Y. Huang, L. Wu, X. Wu, L. Li, L. Chen, Y. Zhang, *J. Am. Chem. Soc.* 137 (2010) 12788–12789.
- [19] X. Chen, Y. Zhao, X. Chang, J. Zuo, H. Zang, W. Xiao, *J. Solid State Chem.* 179 (2006) 3911–3918.
- [20] Z. Yu, Z. Shi, Y. Jiang, H. Yuan, J. Chen, *Chem. Mater.* 14 (2002) 1314–1318.
- [21] *SAINT-Plus*, version 6.02A; Bruker Analytical X-ray Instruments, Inc.: Madison, WI, 2000.
- [22] G.M. Sheldrick, *SHELXTL*, version 6.14; Bruker Analytical X-ray Instruments, Inc.: Madison, WI, 2003.
- [23] A.L. Spek, *Single-crystal structure validation with the program PLATON*, *J. Appl. Crystallogr.* 36 (2003) 7–13.
- [24] G. Zhang, Y. Wu, Y. Li, F. Chang, S. Pan, P. Fu, C. Chen, *J. Cryst. Growth* 275 (2005) e1997–e2001.
- [25] X. Chen, M. Li, X. Chang, H. Zang, W. Xiao, *J. Solid State Chem.* 180 (2007) 1658–1663.